Behavioral/Systems/Cognitive

α4* Nicotinic Receptors in preBötzinger Complex Mediate Cholinergic/Nicotinic Modulation of Respiratory Rhythm

Xuesi M. Shao,[1] Wenbin Tan,[1] Joanne Xiu,[2] Nyssa Puskar,[2] Carlos Fonck,[2] Henry A. Lester,[2] and Jack L. Feldman[1]

[1]Department of Neurobiology, David Geffen School of Medicine at University of California, Los Angeles, Los Angeles, California 90095-1763, and [2]Division of Biology, California Institute of Technology, Pasadena, California 91125

Acetylcholine and nicotine can modulate respiratory patterns by acting on nicotinic acetylcholine receptors (nAChRs) in the preBötzinger complex (preBötC). To further explore the molecular composition of these nAChRs, we studied a knock-in mouse strain with a leucine-to-alanine mutation in the M2 pore-lining region (L9′A) of the nAChR α4 subunit; this mutation renders α4-containing receptors hypersensitive to agonists. We recorded respiratory-related rhythmic motor activity from hypoglossal nerve (XIIn) and patch-clamped preBötC inspiratory neurons in an *in vitro* medullary slice preparation from neonatal mice. Nicotine affected respiratory rhythm at concentrations ∼100-fold lower in the homozygous L9′A knock-in mice compared with wild-type mice. Bath application of 5 nM nicotine increased the excitability of preBötC inspiratory neurons, increased respiratory frequency, and induced tonic/seizure-like activities in XIIn in L9′A mice, effects similar to those induced by 1 μM nicotine in wild-type mice. In L9′A mice, microinjection of low nanomolar concentrations of nicotine into the preBötC increased respiratory frequency, whereas injection into the ipsilateral hypoglossal (XII) nucleus induced tonic/seizure-like activity. The α4*-selective nAChR antagonist dihydro-β-erythroidine produced opposite effects and blocked the nicotinic responses. These data, showing that nAChRs in the preBötC and XII nucleus in L9′A mice are hypersensitive to nicotine and endogenous ACh, suggest that functional α4* nAChRs are present in the preBötC. They mediate cholinergic/nicotinic modulation of the excitability of preBötC inspiratory neurons and of respiratory rhythm. Furthermore, functional α4* nAChRs are present in XII nucleus and mediate cholinergic/nicotinic modulation of tonic activity in XIIn.

Key words: L9′A knock-in mice; α4 subunit; preBötzinger complex; inspiratory neurons; hypoglossal nucleus; nicotine

Introduction

Cholinergic modulation of the neuronal excitability in the pre-Bötzinger complex (preBötC) affects respiratory rhythm and is mediated by both muscarinic acetylcholine receptors (AChRs) and nicotinic AChRs (nAChRs) (Shao and Feldman, 2000, 2001; Bellingham and Ireland, 2002). The nAChRs are of particular interest because they also mediate the effects of exogenously administered nicotine, e.g., via cigarette smoke. Activation of nAChRs in the preBötC affects the excitability of preBötC inspiratory neurons [a subset of these neurons is hypothesized to generate respiratory rhythm (Gray et al., 1999; Feldman et al., 2003)] and perturbs respiratory rhythm (Shao and Feldman, 2001, 2005). Impairment of the excitability of respiratory neurons and/or neurotransmission in the preBötC may underlie pathophysiology of disorders related to central control of breathing such as sudden infant death syndrome, whose incidence is strongly correlated with maternal smoking (Kinney et al., 1995; Anderson et al., 2005; Mitchell and Milerad, 2006).

α4, α7, and β2 nAChR subunits are present in the rostral ventrolateral medulla, probably including the preBötC (Wada et al., 1989; Dominguez del Toro et al., 1994; Dehkordi et al., 2004). Most α4-containing (α4*) receptors in the mouse brain also contain the β2 subunit (β2*), and vice-versa (Whiteaker et al., 2006). Pharmacological studies suggest that the nAChRs in the preBötC mediating nicotinic modulation of respiratory pattern are of α4β2* subtypes (Shao and Feldman, 2002). However, pharmacological tools to identify the specific molecular compositions of native nAChRs are limited. Genetically engineered nAChR subunit knock-out and knock-in animals provide a powerful approach to determine the subunit compositions of nAChRs and their functional roles in CNS (Champtiaux and Changeux, 2004). Knock-in mouse strains with a point mutation at the Leu9′ position in the M2 pore-lining region of nAChR α4 subunits were developed. The α4L9′A mouse strain was designed and selected to display largely normal physiology and behavior in the absence of added drugs. The strain resembles wild-type with regard to locomotion and ambulation, learning behavior, and anxiety; their neuroanatomy is normal. There are subtle differences from wild-type in their sleep–wake cycle. However, the L9′A mice are strikingly hypersensitive to several effects of nicotine: reward behavior, hypothermia, tolerance to hypothermia, locomotor sensitization, Straub tail, and seizures. This hypersensitivity to agonists is also displayed at the cellular and membrane levels in several preparations (Tapper et al., 2004; Fonck et al., 2005).

These gain-of-function knock-in mouse strains allow tests of the hypothesis that activation of α4* receptors is sufficient to produce a given response (Labarca et al., 2001; Fonck et al., 2003, 2005; Tapper et al., 2004, 2007). Using the L9′A mouse strain, we tested the hypothesis that activation of α4* nAChRs alters the excitability of neurons in the preBötC rhythmogenic network and that these nAChRs can mediate cholinergic/nicotinic modulation of respiratory rhythm. Identifying the molecular composition of nAChRs mediating the cholinergic modulation of respiratory pattern provides molecular basis for developing therapeutic agents targeting nAChRs (Picciotto et al., 2001; Gotti et al., 2006), both protective and interventional, with fewer side effects because of increased specificity.

Materials and Methods

L9′A knock-in mice. These experiments used mice of the L9′A knock-in strain, backcrossed at least 10 generations to C57BL/6. Generation of the L9′A knock-in mice was reported in detail by Tapper et al. (2004) and Fonck et al. (2005). Only homozygous mutant knock-in mice and wild-type C57BL/6 mice were used in this study. The genotype of the mice used in the electrophysiological experiments was confirmed by PCR analysis of tail DNA.

Slice preparation. Experiments were performed on a medullary slice preparation that retains functional respiratory networks and generates respiratory rhythm *in vitro* (Smith et al., 1991). A neonatal mouse [postnatal day 0 (P0)–P3], either wild-type C57BL/6 or L9′A, was anesthetized with isoflurane and then promptly decerebrated. Tissue dissection and slicing were performed in an artificial CSF (ACSF) containing (in mM) 128 NaCl, 3.0 KCl, 1.5 $CaCl_2$, 1.0 $MgSO_4$, 23.5 $NaHCO_3$, 0.5 NaH_2PO_4, and 30 glucose, and equilibrated with 95% O_2–5% CO_2 (pH = 7.4) at room temperature. The cerebellum was removed and the brainstem–spinal cord was isolated. The brainstem–spinal cord was mounted in the specimen vise of a Vibratome (VT 100, Technical Products International, St. Louis, MO) oriented vertically with rostral end upward. The brainstem was sectioned serially in the coronal plane with a dissection microscope until the landmarks, e.g., nucleus ambiguus and inferior olive, at the rostral boundary of the preBötC were visible. One transverse slice (450 –550 μm thick) was cut. The slice was transferred to a recording chamber of 1.2 ml volume and stabilized with a threaded frame. During electrophysiological recordings, the slice was continuously perfused (2 ± 0.5 ml/min) with ACSF with increased KCl (9 mM) equilibrated with 95% O_2–5% CO_2. The ACSF in the recording chamber was maintained at 27 ± 1°C. All slices studied spontaneously generated respiratory rhythm at these conditions and the respiratory-related rhythmic activity can be recorded from the XIIn (Smith et al., 1991).

L9′A mutation expressed in Xenopus *oocytes.* Wild-type rat α4 and β2 nicotinic subunits were subcloned in the pAMV vector. The Quikchange kit (Stratagene, La Jolla, CA) was used to construct the α4L9′A mutations, which were verified by DNA sequencing. Capped cRNA was synthesized from linearized cDNA using the mMessage mMachine RNA transcription kit (Ambion, Austin, TX).

Stage V–VI *Xenopus* oocytes were surgically isolated, and surgeries performed, using methods approved by the Caltech Institutional Animal Care Committee. Isolated oocytes were injected with 4 ng of mutated α4 and 4 ng of wild-type β2 cRNA in 50 nl of H_2O. Before recording, injected oocytes were incubated for 2 d in a solution containing (in mM) 96 NaCl, 5 HEPES, 2.5 Na pyruvate, 2 KCl, 1.8 $CaCl_2$, 1 $MgCl_2$, 2.5 μg/ml gentamycin, and 5% horse serum, pH 7.4, at 18°C.

Electrophysiological recording. Neurons within 100 μm of the slice surface were visualized with an infrared-differential interference contrast microscope (Axioskop2, Carl Zeiss, Göttingen, Germany). The respiratory neurons we recorded fired in phase with the inspiratory bursts of the XIIn rhythmic motor output and were located ventral to the nucleus ambiguus in the preBötC. Patch pipettes were pulled from thick wall (0.32 mm) borosilicate glass with tip size 1–1.5 μm (resistance: 4 –6.5 MΩ). The pipette filling solution contained (in mM) 135 K-gluconate, 5.0 NaCl, 0.1 $CaCl_2$, 1.1 EGTA, 10 HEPES, 2.0 ATP (Mg^{2+} salt), and 0.3 GTP

(Na$^+$ salt), pH adjusted to 7.25 with KOH. To maintain stable electrode potentials during whole-cell patch-clamp recordings, a micro-agar salt bridge of 3 M KCl was built in the electrode holder that formed an electrical connection between the pipette solution and the Ag/AgCl wire connected to the headstage of a patch-clamp amplifier (Shao and Feldman, 2007a). Intracellular signals were amplified and low-pass filtered at 2 kHz with a patch-clamp amplifier (MultiClamp 700B, Molecular Devices, Sunnyvale, CA). A −10 mV junction potential was determined experimentally; reported potential values are corrected for junction potential. For experiments in which drugs were bath applied, only one neuron was recorded from each preparation to avoid confounding effects of drug residue.

Respiratory-related rhythmic motor activity was recorded from the cut ends of XIIn with a suction electrode, amplified (20,000×), and bandpass filtered (1 Hz to 3 kHz) with an amplifier (P5 series, Grass Instruments, Quincy, MA). Signals from intracellular recordings and from XIIn were digitized at 10 kHz sampling frequency with the Digidata 1440A and software CLAMPEX 10 (Molecular Devices) on a Pentium-based computer. The two channels of signals were saved as data files for further analyses off-line.

We used an automated parallel two-electrode voltage-clamp (OpusXpress, Molecular Devices) to measure the agonist-induced currents in injected oocytes at −60 mV. During recordings, oocytes were continually superfused with a nominally Ca^{2+}-free saline (ND96) containing the following (in mM): 96 NaCl, 5 HEPES, and 1 $MgCl_2$, pH 7.4, to prevent activation of the endogenous Ca^{2+}-activated Cl^- current. Test solutions were applied at rate of 4 ml/s (chamber volume, ~0.5 ml).

Drug application. Drugs were applied in two different ways: (1) bath application, i.e., adding them to the perfusate. In this procedure, stable recordings from a respiratory neuron and from XIIn can be obtained, and the drug concentrations for the slice are known accurately (drugs take effect in 2–4 min after adding them to the perfusate in our perfusion system); (2) pressure microinjection into the preBötC or XII nucleus. In this procedure, the location of drug action can be precisely identified. We estimate 1:10 reduction on average in drug concentration from the injection pipette to the target region (Liu et al., 1990). For microinjection experiments, a 5 μl calibrated glass pipette (Drummond Scientific, Broomall, PA) was pulled, and the tip was broken to 6–9 μm in diameter. The back of the pipette was connected to an air pressure source of 55– 85 kPa. The pipette was mounted on a micromanipulator and advanced into the preBötC or XII nucleus, 100–200 μm below the slice surface. The injection volume was monitored by the displacement of the fluid meniscus using a microscope with a calibrated eyepiece reticule. A volume of 10 nl was injected, which is estimated to diffuse to a region approximating the size of the preBötC within 10 s (Nicholson, 1985). For injections into XII nucleus, 15–20 nl was injected. Drugs were dissolved in a pipette solution containing (in mM) 150 NaCl, 9 KCl, 1.5 $CaCl_2$, 1.0 $MgSO_4$, 10 HEPES, and 30 glucose, pH adjusted to 7.4 with NaOH.

For bath application of cholinergic drugs, the effects were measured 3–5 min after addition. The recordings of the neuronal and XIIn activity immediately before drug application served as controls for each preparation.

(−)-Nicotine (hydrogen tartrate salt) and dihydro-β-erythroidine hydrobromide (DHβE) were obtained from Sigma (St. Louis, MO).

Data analysis. The respiratory-related motor activity recorded from XIIn was digitally integrated by full-wave rectification and low-pass filtering (digital RC filter) at a time constant of 40 ms using a data analysis software DataView V4.7 (W. J. Heitler, University of St. Andrews, St. Andrews, UK). The intracellular signals were digitally low-pass filtered at 1150 Hz (eight-pole Bessel filter) except for measuring the phasic inward current of inspiratory neurons, for which the intracellular signal was filtered at 20 Hz. Respiratory periods were averaged from 10 consecutive periods in control or drug application conditions for each preparation, except in the microinjection experiments, in which 7–10 consecutive periods were averaged, as the nicotine effects were briefer after microinjection. Because the distribution of periods is Gaussian, periods were averaged across preparations for statistical tests. Respiratory frequency was taken as reciprocal of period and presented as mean ± SD in the text. The amplitude (and duration) of integrated inspiratory bursts of XIIn
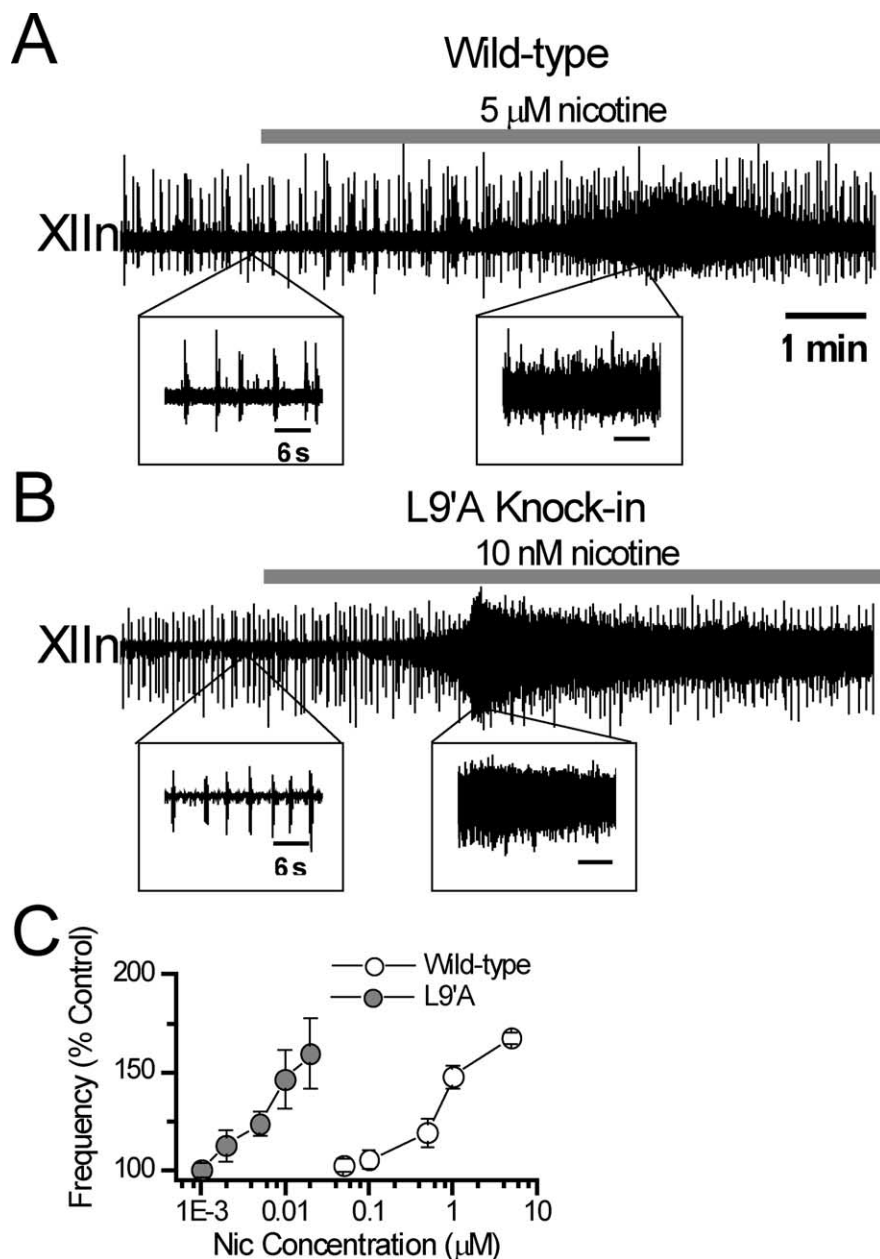
Figure 1. Nicotine (Nic) at low nanomolar concentrations increased frequency of respiratory rhythm and induced intense tonic/seizure-like activity in L9′A mice compared with effects of Nic at micromolar concentrations in wild-type mice *in vitro*. ***A***, Respiratory-related rhythmic activity recorded from the hypoglossal nerve roots (XIIn) in the medullary slice preparation of a wild-type mouse in response to bath application of 5 μM Nic. Insets, Activities on an expanded time scale. ***B***, Respiratory-related rhythmic activity from a slice of nAChR α4 subunit L9′A knock-in mouse in response to bath application of 10 nM Nic. Time scales are equivalent for ***A*** and ***B***. Time scales for all insets are equivalent. ***C***, Concentration dependence of respiratory frequency in L9′A and wild-type mice. Percentage (%) control of frequency = 100 × (frequency at the test Nic concentration)/(frequency in pre-Nic conditions). Data were averaged across preparations (*n* = 3–12) and presented as mean ± SE.

experiments with the antagonist DHβE followed by nicotine, we measured electrophysiological parameters before and during application of DHβE and during nicotine + DHβE for each neuron in each slice. One-way repeated-measures ANOVA was used to test the statistical significance for drug treatments. *Post hoc* comparison analyses based on Tukey were used to determine the significance of differences between DHβE application and control and between nicotine + DHβE and DHβE alone. The procedure MIXED in the data analysis software package SAS (V9, SAS Institute, Cary, NC) was used for these analyses. In all analyses, $p \leq 0.05$ was the criterion for statistical significance.

Membrane noise (current fluctuation of voltage-clamped inspiratory neurons) and spontaneous EPSCs (sEPSCs) during expiratory periods were analyzed with DataView 4.7. Membrane noise was quantified by calculating root-mean-square (rms, statistically equivalent to SD calculation) of the current recordings (inspiratory periods were excluded) at a bandwidth of 1–1000 Hz. Recording sections of 1–2 min that contained 200–2000 sEPSCs were taken from predrug control and drug application conditions. The program detected sEPSCs during expiratory periods by an optimally scaled template recognition algorithm (Clements and Bekkers, 1997). Rate, i.e., frequency of sEPSCs was determined by dividing the number of sEPSCs by total expiratory duration (inspiratory periods were subtracted) in the 1–2 min sections from predrug and drug application conditions. Then they were averaged across neurons. Differences in mean rates were tested with paired *t* test or repeated-measures ANOVA as described above. sEPSC amplitude was analyzed with one-way repeated-measures ANOVA taking every sEPSC in the 1–2 min sections from predrug and drug application conditions recorded from an individual neuron as repeated measurements.

Results

Respiratory rhythm of L9′A mice is hypersensitive to nicotine at low nanomolar concentrations *in vitro*

Respiratory-related rhythmic activity was recorded from XIIn in *in vitro* medullary slice preparations of wild-type and L9′A mice. In slices from L9′A mice, the frequency of rhythmic activity increased in response to bath application of nanomolar concentrations of nicotine, in contrast to the micromolar concentrations required to elicit responses in slices from wild-type mice (Fig. 1*A*,*B*). The nicotine concentration–frequency response curve in L9′A mice was greatly left-shifted compared with that of wild type. Equipotent effects of nicotine occurred at concentrations ∼100-fold lower in L9′A than in wild-type slices (Fig. 1*C*), suggesting that the nAChRs in L9′A mice are hypersensitive to nicotine and that the nAChRs mediating the modulatory effects on the respiratory pattern contain α4 subunits. In slices from L9′A mice, low nanomolar concentrations of nicotine also induced tonic/seizure-like activity, an effect seen in wild-type mice only at micromolar nicotine (Fig.

and the inspiratory drive current of inspiratory neurons were measured from the averaged envelope of five to six consecutive inspiratory periods triggered by the up stroke of the integrated inspiratory XIIn bursts (Data-View 4.7). Durations were measured at 20% of peak amplitude. Then, they were averaged across neurons or preparations and presented as mean ± SD, except when indicated as mean ± SE in the figures. *n* = number of cells (for whole cell recording) or preparations (for XIIn motor output recording) is indicated in the text. For experiments with application of nicotine, paired *t* tests (except as indicated otherwise) for significance were applied taking the measurements before (predrug control) and during nicotine application as a pair for each preparation. For

1A,B). The intense tonic/seizure-like activities vitiated systematic frequency measurements for increases more than ~50%; therefore, we did not calculate EC_{50} values. To insure inducing significant responses while avoiding intense seizure-like activity in the subsequent cellular experiments, we used 5 nM nicotine for L9′A preparations and 1 μM nicotine for wild-type preparations.

In control conditions without nicotine application, the respiratory frequency of preparations from L9′A mice was higher than that from wild-type mice. Mean respiratory frequency of L9′A slice was 11.9 ± 2.9 inspiratory bursts/min versus 9.8 ± 3.2/min in wild-type ($p = 0.018$, nonpaired t test, $n = 33$ vs $n = 29$). This result suggests that the hypersensitive L9′A nAChRs are tonically responding to the endogenous ligands, such as ACh, spontaneously released from presynaptic structures in slices.

Reponses of preBötC inspiratory neurons of L9′A mice to nicotine at low nanomolar concentrations

To test the hypothesis that nicotine acting via α4* nAChRs depolarizes preBötC neurons producing increases in respiratory frequency, we recorded membrane potentials from whole-cell current-clamped preBötC inspiratory neurons in the slice preparations. These neurons discharge in synchrony with the respiratory-related rhythmic motor activity simultaneously recorded from XIIn. We applied hyperpolarizing current to maintain preBötC inspiratory neurons at a baseline membrane voltage of −70 to −65 mV in the absence of drug. Bath application of 5 nM nicotine to slices from L9′A mice depolarized these neurons and induced tonic spiking (Fig. 2). At the same time, nicotine increased the frequency of respiratory-related rhythmic activity and induced tonic activity, as shown by the elevated baseline between inspiratory bursts in the integrated XIIn traces (∫XIIn, $n = 3$). The neuron shown in Figure 2 was a pacemaker neuron that fired ectopic bursts (indicated by arrows in the insets) during expiratory periods. In agreement with previous data (Shao and Feldman, 2002), we observed similar responses with a nicotine concentration of 1 μM in wild-type slices (data not shown). Addition of 0.2 μM DHβE reversed these effects; it hyperpolarized inspiratory neurons and produced a corresponding decrease in the respiratory frequency and suppressed the tonic activity in XIIn (Fig. 2). The fact that the frequency fell below the predrug control level with nicotine plus DHβE suggests that there is endogenous ACh release in the preBötC acting on the hypersensitive α4* nAChRs to modulate respiratory rhythm. DHβE applied in the presence of nicotine blocked both the effects of nicotine and the effects of endogenous ACh on the knock-in α4* nAChRs.

For more quantitative analysis of neuronal responses, we recorded from preBötC inspiratory neurons in voltage-clamp mode (holding potential $V_h = −65$ mV). With slices from wild-type mice, application of 1 μM nicotine increased respiratory frequency from 9.2 ± 3.0/min to 13.5 ± 4.1/min ($p < 0.001$, $n = 12$) without affecting the amplitude of integrated XIIn rhythmic
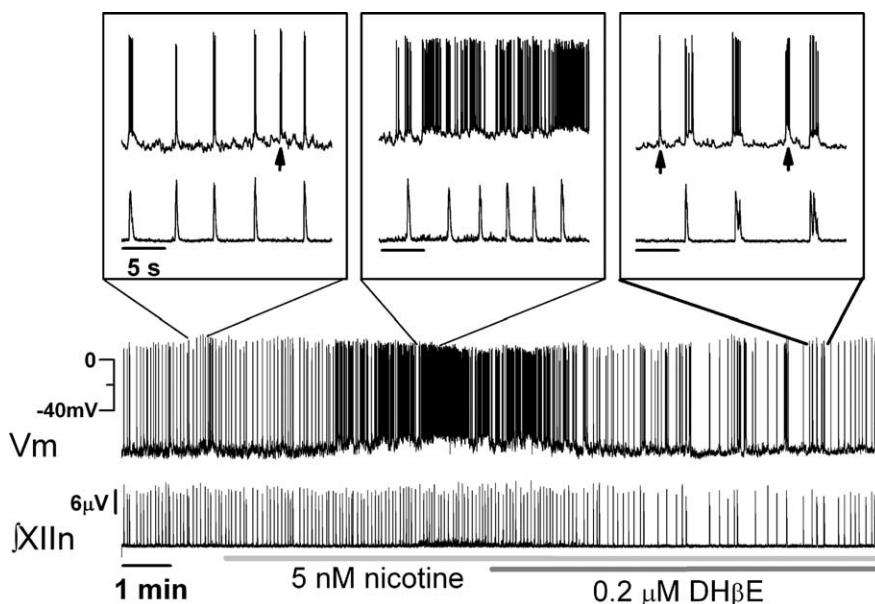

Figure 2. Nicotine (5 nM, bath applied) depolarized preBötC inspiratory neurons and increased respiratory frequency in L9′A mouse slices; effects were blocked by DHβE (0.2 μM). Simultaneous whole-cell patch-clamp recording from an inspiratory neuron (top trace) in the preBötC and extracellular recording from the XIIn (∫XIIn: integrated nerve activity) in a medullary slice. The neuron was current clamped at −16 pA to keep the baseline membrane voltage (V_m) at −70 to −65 mV before nicotine application. The neuron fired bursts of action potentials on top of rhythmic inspiratory depolarization synchronized with the rhythmic motor activity of XIIn. Note that this neuron also fired a number of bursts of action potentials during expiratory periods (arrows in insets) indicating pacemaker properties. Insets, Activities of both channels on an expanded time scale at time sections indicated. Time scales for all insets are equivalent. y-Scales for the continuous recordings and all the insets are equivalent for corresponding channels.

activity (10.4 ± 12.9 μV in control, i.e., prenicotine conditions vs 9.6 ± 12.0 μV in the presence of nicotine, $p = 0.89$, $n = 12$) (Fig. 3A,B,E). In the voltage-clamped neurons, nicotine induced (1) a tonic inward current of 17.3 ± 10.8 pA (measured as baseline current during expiratory periods during nicotine application minus baseline current in prenicotine conditions; $p = 0.005$, $n = 7$) associated with an increase in membrane noise (current fluctuation) [rms value of the membrane noise increased from 4.47 ± 1.37 to 6.42 ± 1.47 pA ($p = 0.0084$, $n = 5$) (Fig. 3A,F). Membrane noise consists of extrasynaptic channel activity, including ligand-gated and voltage-gated channels, resolved and unresolved sEPSCs and sIPSCs, and random noise. A tonic inward current associated with an increase in membrane noise suggests predominantly excitatory extrasynaptic and/or synaptic channel activation.]; (2) a decrease in amplitude of phasic inspiratory drive current from 65.1 ± 47.4 to 56.3 ± 44.0 pA ($p = 0.01$, $n = 11$) and duration from 447 ± 111 to 388 ± 125 ms (measured at 20% of peak, $p = 0.032$) (Fig. 3B,F); (3) an increase in frequency of sEPSCs during expiratory periods from 10.9 ± 5.0/s to 14.7 ± 6.0/s ($p = 0.012$, $n = 6$) and an increase in amplitude of sEPSCs from −13.0 ± 3.3 to −15.1 ± 3.6 pA ($p = 0.0002$) (Fig. 3A, insets, F). Figure 3, E and F, shows the summary data of XIIn activity and single neuron parameters respectively as percentage changes referred to prenicotine application. These responses slightly desensitized when nicotine was present for >6 min.

With L9′A slices, bath application of 5 nM nicotine increased respiratory frequency from 12.4 ± 1.9/min to 15.3 ± 3.1/min ($p = 0.002$, $n = 9$) without affecting the amplitude of integrated XIIn rhythmic activity (7.1 ± 5.2 μV in prenicotine control conditions vs 7.7 ± 5.0 μV in the presence of nicotine, $p = 0.21$, $n = 8$) (Fig. 3C–E). In the voltage-clamped neurons, 5 nM nicotine
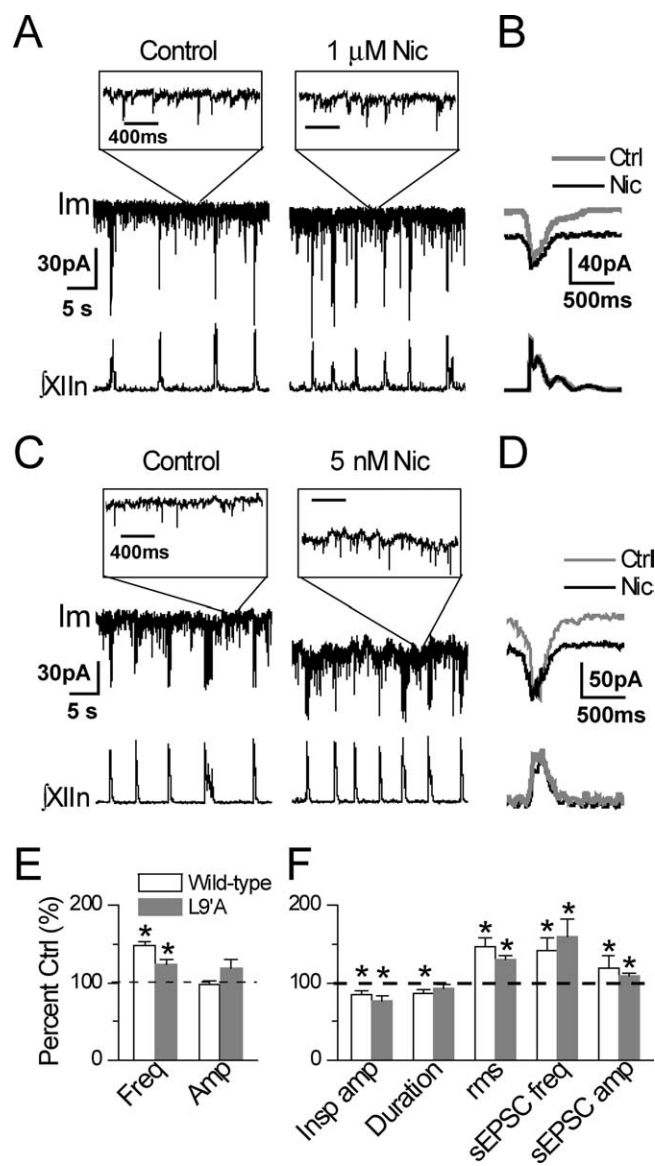
Figure 3. Responses of voltage-clamped preBötC inspiratory neurons and XIIn rhythmic activity to nicotine (Nic) application in L9′A and wild-type mice. **A**, A preBötC inspiratory neuron and the respiratory-related XIIn rhythmic motor activity in a slice preparation from a wild-type mouse in the absence (left) and presence (right) of bath-applied 1 μM Nic. I_m is membrane current of the neuron (holding potential $V_h = -65$ mV). ∫XIIn, Integrated XIIn activity. Insets, I_m recordings on an expanded time scale at time sections indicated, revealing sEPSCs. Time scales for the two insets are equivalent. y-Scales for the continuous recordings and all the insets are equivalent. **B**, Phasic inspiratory drive current of a preBötC inspiratory neuron. Averaged envelopes of five to six consecutive inspiratory periods for both I_m and ∫XIIn channels in Nic application versus pre-Nic control (Ctrl) conditions. I_m traces were low-pass filtered at 20 Hz. Average was triggered by the up strokes of the integrated inspiratory bursts from XIIn. Duration of inspiratory drive current was measured at 20% of peak amplitude. Traces were from recordings of a different slice from those of **A**. **C**, As in **A**, a preBötC inspiratory neuron and the XIIn rhythmic activity in a slice preparation from an L9′A mouse in the absence (left) and presence (right) of bath applied 5 nM Nic. **D**, As in **B**, phasic inspiratory drive current of a preBötC inspiratory neuron from an L9′A slice. **E**, Summary data (mean ± SE) of XIIn rhythmic activity for L9′A mice in response to 5 nM Nic versus wild-type mice in response to 1 μM Nic. Freq, Frequency; Amp, amplitude. **F**, Summary data of preBötC inspiratory neurons of L9′A mice in response to 5 nM Nic versus wild-type mice in response to 1 μM Nic applications. Insp amp, Phasic inspiratory drive current amplitude; Duration, duration of inspiratory drive current; rms, root-mean-square of membrane noise during expiratory periods; sEPSC freq, spontaneous EPSC frequency during expiratory periods: number of sEPSCs divided by total expiration time during 1–2 min recording time sections. Each section contained 200–2000 sEPSCs. *$p \leq 0.05$ between Nic application and pre-Nic control. Numbers of neurons or preparations (n) for each experiment are indicated in the text of Results.

induced (1) a tonic inward current of 34.8 ± 29.7 pA ($p = 0.035$, $n = 6$) associated with an increase in membrane noise (rms value from 5.62 ± 2.11 to 7.34 ± 2.57 pA, $p = 0.0046$, $n = 5$) (Fig. 3C,F); (2) a decrease in the amplitude of inward phasic inspiratory drive current from 103.2 ± 149.3 to 90.7 ± 149.0 pA ($p = 0.049$, $n = 6$) without affecting the duration (421 ± 117 ms in control conditions vs 383 ± 78 ms in the presence of nicotine, $p = 0.28$, $n = 5$) (Fig. 3D,F); (3) an increase in the frequency of sEPSCs during expiratory periods from 10.5 ± 5.5/s to 15.3 ± 6.4/s ($p = 0.015$, $n = 5$) and an increase in amplitude of sEPSCs from −17.7 ± 4.9 to −19.3 ± 5.4 pA ($p = 0.0037$) (Fig. 3C, insets, F). Figure 3, E and F, shows the summary data for XIIn activity and single neuron parameters respectively as percentage changes referred to prenicotine application as controls. These responses slightly desensitized when nicotine was present for >6 min.

These results show that the nAChRs mediating nicotinic effects on inspiratory neurons in the preBötC rhythmogenic network in L9′A mice are hypersensitive to nicotine; therefore, these nAChRs contain α4 subunits. Activation of α4* nAChRs facilitates excitatory glutamatergic input to these neurons and induces a tonic inward current that enhances the excitability of the neurons. Depolarization of these neurons results in increased respiratory frequency.

DHβE blocks the nicotine effects on preBötC inspiratory neurons and on respiratory rhythm and induces opposite effects in L9′A mice

The effects of nicotine on preBötC inspiratory neurons and on the pattern of respiratory-related motor activity in neonatal rats can be blocked by DHβE (Shao and Feldman, 2002), a selective antagonist of α4* nAChRs, although not completely specific (Harvey and Luetje, 1996; Harvey et al., 1996). We tested whether this antagonist blocks the effects of low nanomolar concentrations of nicotine on preBötC inspiratory neurons and respiratory rhythm in L9′A slices by applying DHβE before exposure to nicotine. Bath application of DHβE (0.1–0.2 μM) decreased frequency from 10.2 ± 3.0/min to 5.5 ± 2.4/min ($p = 0.033$, $n = 4$) with no significant effect on the amplitude of integrated inspiratory bursts of XIIn motor output (7.6 ± 6.9 μV in control conditions vs 8.0 ± 7.5 μV in the presence of DHβE, $p = 0.65$, $n = 4$) (Fig. 4A–C). In contrast to nicotine, DHβE alone induced (1) a tonic outward current of 8.3 ± 2.5 pA ($p = 0.028$, $n = 3$) associated with a decrease in rms value of membrane noise from 6.26 ± 2.89 to 4.10 ± 1.52 pA ($p = 0.022$, $n = 4$) (Fig. 4A,D); (2) a statistically insignificant increase in amplitude of phasic inspiratory drive current from 67.6 ± 47.0 to 74.8 ± 52.2 pA ($p = 0.43$) and in duration from 475 ± 162 ms to 560 ± 184 ms ($p = 0.41$, $n = 4$) (Fig. 4B,D); (3) a decrease in frequency of sEPSCs during expiratory periods from 16.7 ± 11.1/s to 8.7 ± 4.5/s ($p = 0.023$) and in amplitude of sEPSCs from −17.4 ± 5.4 to −13.9 ± 2.5 pA ($p < 0.001$, $n = 4$) (Fig. 4A,D). The results that application of DHβE alone produced effects opposite to those of nicotine in L9′A slices suggest that there is endogenous ligand release, such as ACh, in the preBötC, acting on the hypersensitive α4* nAChRs to modulate respiratory rhythm. Evidently the hypersensitive nAChRs are not completely desensitized by the background levels of endogenous ACh, consistent with the finding that the hypersensitive receptors have a "window" of activation in the sustained presence of agonist (Fonck et al., 2005).

Subsequent addition of nicotine (5 nM) in the presence of DHβE did not have further effect on respiratory rhythm and on most parameters measured in preBötC inspiratory neurons. Application of nicotine induced insignificant changes in respiratory
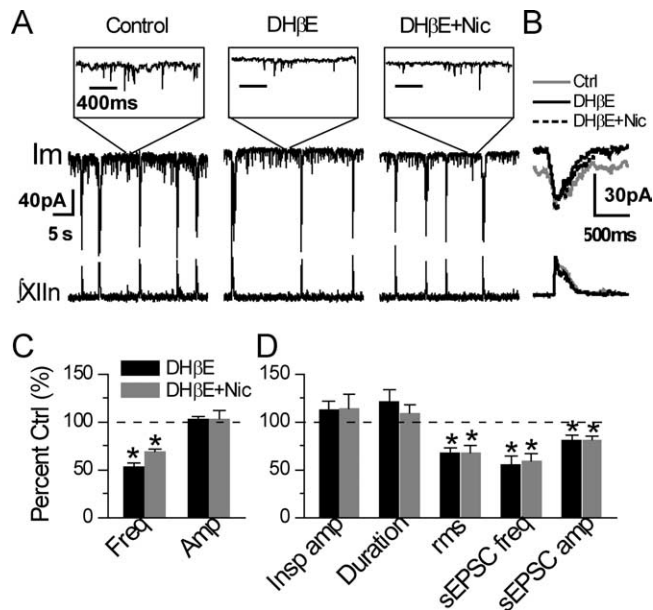
Figure 4. α4* selective nicotinic antagonist DHβE induced opposite effects and blocked the effects of nicotine (Nic) on preBötC inspiratory neurons and on the XIIn rhythmic activity in L9′A mice. *A*, preBötC inspiratory neuron and respiratory-related XIIn rhythmic activity in a L9′A slice in response to bath application of 0.2 μM DHβE followed by 5 nM Nic in the presence of DHβE (DHβE + Nic). I_m, Membrane current of the neuron ($V_h = -65$ mV). ∫XIIn, Integrated XIIn activity. Insets, I_m recordings on an expanded time scale at time sections indicated to show sEPSCs. Time scales for the three insets are equivalent. *y*-Scales for the continuous recordings and the insets are equivalent. *B*, Phasic inspiratory drive current of a preBötC inspiratory neuron from a different slice. Averaged envelopes of five to six consecutive inspiratory periods for both I_m and ∫XIIn traces in the conditions of predrug control (Ctrl), DHβE application, and DHβE + Nic. I_m traces were low-pass filtered at 20 Hz. Average was triggered by the up strokes of the integrated inspiratory bursts from XIIn. Durations of inspiratory drive current were measured at 20% of peak amplitude. *C*, Summary data (mean ± SE) of XIIn rhythmic activity of L9′A in response to 0.2 μM DHβE application followed by DHβE + Nic. Freq, Frequency; Amp, amplitude. *D*, Summary data of preBötC inspiratory neurons in response to DHβE followed by DHβE + Nic. Insp amp, Phasic inspiratory drive current amplitude; Duration, duration of inspiratory drive current; rms, root-mean-square of membrane noise during expiratory periods; sEPSC freq, spontaneous EPSC frequency during expiratory periods: number of sEPSCs divided by total expiration time during 1–2 min recording times. *$p \leq 0.05$, statistical significance between drug application and predrug control.

frequency to 6.9 ± 1.6/min ($p = 0.19$, $n = 4$) and in amplitude of inspiratory bursts to 8.0 ± 7.8 μV ($p = 0.998$) (Fig. 4*A,C*). In voltage-clamped inspiratory neurons, nicotine induced insignificant changes in tonic outward current to 9.8 ± 9.2 pA ($p = 0.78$, $n = 3$) and in membrane noise to 4.29 ± 2.11 pA ($p = 0.94$, $n = 4$) (Fig. 4*A,D*), insignificant changes in amplitude of phasic inspiratory drive current to 75.4 ± 53.8 pA ($p = 0.99$) and in duration to 507 ± 154 ms ($p = 0.68$, $n = 4$) (Fig. 4*B,D*), and insignificant changes in frequency of sEPSCs during expiratory periods to 9.9 ± 6.5/s ($p = 0.68$, $n = 4$) and in amplitude of sEPSC to -14.0 ± 4.2 ($p = 0.27$) (Fig. 4*A,D*).

These results show that the nicotine effects at nanomolar concentrations on preBötC inspiratory neurons and respiratory rhythm in L9′A slices can be blocked by DHβE. These results are consistent with the hypothesis that α4* nAChRs mediate cholinergic/nicotinic modulation of the excitability of preBötC inspiratory neurons and regulation of respiratory rhythm.

DHβE blocks the responses of (α4L9′A) β2 nAChRs to nicotine and ACh

To test whether DHβE remains a potent antagonist for L9′A mutated receptors, we expressed (α4L9′A)β2 receptors in oo-
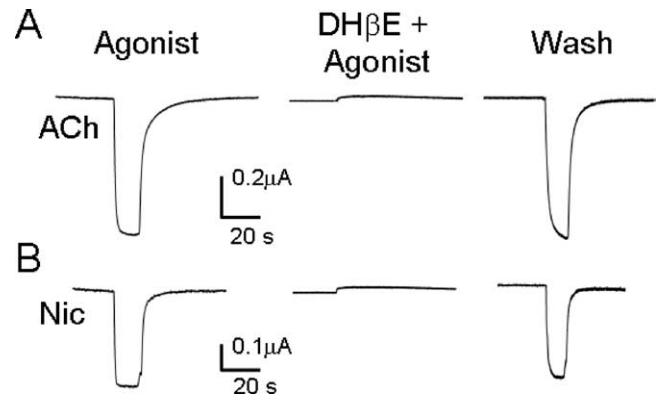
Figure 5. Reversible block of (α4L9′A)β2 receptors expressed in oocytes by 0.2 μM DHβE. *A, B*, Agonist concentration in each case was the EC_{20} for ACh (0.125 μM, *A*) or Nic (0.025 μM, *B*), applied for 15 s. Left, first agonist application. Oocytes were washed with recording buffer for 2 min (not shown) and then perfused with 0.2 μM DHβE for 5 min. Middle, The subsequent response to coapplied agonist + 0.2 μM DHβE. Oocytes were then washed with buffer for 5 min, and an additional 15 s application of agonist was given (right). These data are typical of $n > 5$ oocytes for each agonist. The small outward deflections are solution change artifacts.

cytes. Because DHβE had modest effects on the rhythmic activity and sEPSC frequency in the slice preparation (Fig. 4), we inferred that DHβE blocked the effect of endogenous ACh, presumably at concentrations that were well below saturating levels. We therefore tested agonists (ACh or nicotine) at their EC_{20} (0.125 and 0.025 μM, respectively, verified during the present experiments) (Fonck et al., 2005). The agonist-induced currents were completely and reversibly blocked by 0.2 μM DHβE (Fig. 5). These results suggest that DHβE is still a potent blocker for the hypersensitive α4L9′A nAChRs (as it is for wild-type α4β2 receptors). These results are also consistent with a previous oocyte expression study: DHβE remains a potent blocker when α4 Leu9′Thr, an even more hypersensitive mutation than the present L9′A mutation, is incorporated into the α4 subunit of α4β2 nAChRs (Moroni et al., 2006).

α4* nAChRs in the preBötC mediate nicotinic modulation of respiratory rhythm, and these receptors in the XII nucleus mediate nicotinic effects on the tonic activity

In slice preparations, we can pressure inject determined volumes of drugs into precisely located regions. To test whether the preBötC is responsible for the nicotinic modulation of respiratory rhythm via α4* nAChRs, we microinjected nicotine at appropriately low concentrations locally into the preBötC in L9′A slices and recorded the respiratory-related rhythmic motor activity from XIIn. For comparison, we also injected nicotine into the XII nucleus.

Unilateral microinjection of 50 nM nicotine (10–15 nl; refer to Materials and Methods section) increased respiratory frequency from 9.8 ± 1.8/min to 14.2 ± 2.9/min ($p < 0.001$, $n = 9$) (Fig. 6*A*). These microinjections did not affect the amplitude (15.0 ± 5.5 μV in prenicotine control conditions vs 13.9 ± 4.6 μV after nicotine injection, $p = 0.07$, $n = 9$) of integrated inspiratory bursts of XIIn motor output (Fig. 6*A,B*). Similar effects on frequency were observed after either ipsilateral or contralateral microinjection of nicotine. Bath application of 0.1–0.5 μM DHβE greatly reduced the frequency effect induced by nicotine injection into the preBötC (8.6 ± 1.9/min in prenicotine conditions vs 10.1 ± 1.2/min after nicotine injection; $p = 0.074$, $n = 6$). Nicotine injection did not affect the peak amplitude of integrated XIIn rhythmic motor activity (11.8 ± 6.8 μV in prenicotine condi-
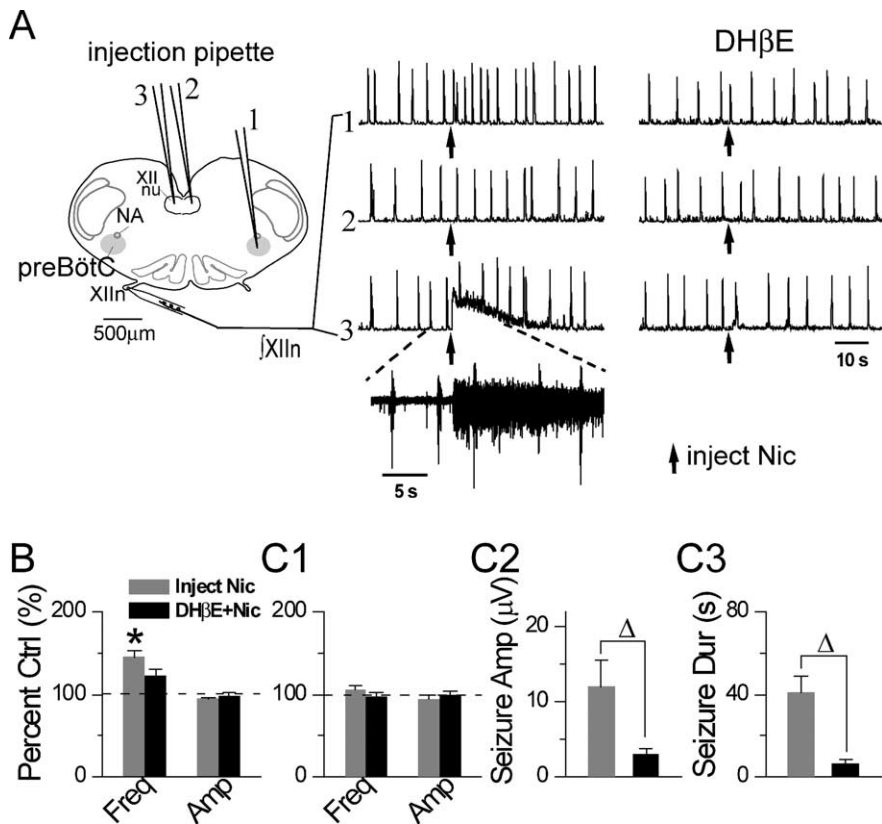
Figure 6. Microinjection of low nanomolar concentrations of nicotine (Nic) into the preBötC increased the frequency of respiratory-related XIIn rhythmic activity, and into hypoglossal nucleus (XII nu) induced tonic/seizure-like activity in L9′A mice. DHβE greatly reduced these effects. **A**, Microinjection locations, the responses to Nic injections recorded from XIIn in the absence (middle) and presence (right) of bath-applied DHβE (0.1–0.5 μM). Trace 1, Injection of 50 nM Nic (10–15 nl) into contralateral preBötC corresponding to the injection pipette #1. Trace 2, Injection of Nic (15–20 nl) into contralateral XII nu corresponding to the injection pipette #2. Trace 3, Injection of Nic (15–20 nl) into ipsilateral XII nu corresponding to the injection pipette #3. ∫XIIn, Integrated XIIn activity. Inset, Raw (nonintegrated) XII activity on an expanded time scale from the indicated section of trace 3 showing seizure-like activity. Injection pipettes were inserted into the target areas 100–200 μm below the surface of the slice. Arrow indicates the time of Nic injection. **B**, Summary data (mean ± SE) of frequency (Freq) and amplitude (Amp) of integrated XIIn rhythmic activity in response to Nic injection into the preBötC in the absence and presence of bath applied DHβE. Amplitude was determined with averaged envelopes of five to six consecutive inspiratory bursts for each condition. **C**, Summary data of the effects of Nic injection into ipsilateral XII nu in the absence and presence of bath-applied DHβE on frequency and amplitude of integrated XIIn rhythmic activity (**C1**), Nic-induced tonic/seizure-like activity amplitude (Seizure Amp; **C2**), and duration (Seizure Dur; **C3**) measured at 20% of peak amplitude of integrated XIIn activity. *Statistically significant difference between Nic injection versus pre-Nic conditions (paired t test). △Statistically significant difference of Nic effects between the absence and presence of bath applied DHβE.

tions vs 11.3 ± 5.4 μV after nicotine injection; $p = 0.47$, $n = 6$) in the presence of DHβE (Fig. 6A,B).

Microinjection of 50 nM nicotine (15–20 nl) into the ipsilateral XII nucleus induced tonic/seizure-like activity (Fig. 6A, trace 3) that had a peak amplitude of 12.0 ± 9.4 μV (integrated nerve recording) and lasted 41.1 ± 21.0 s (measured by decline to 20% of the peak amplitude; $n = 7$) (Fig. 6C2,C3). During these nicotine-induced seizures, the rhythmic inspiratory activity continued at near-control frequency (10.7 ± 1.6/min in prenicotine control conditions vs 11.1 ± 0.9/min after nicotine injection, $p = 0.26$, $n = 7$) and amplitude (13.7 ± 6.6 μV vs 12.9 ± 6.3 μV, $p = 0.28$) (Fig. 6A,C1). There was no effect when nicotine was injected into the contralateral XII nucleus (Fig. 6A, trace 2); this served as a control for nonspecific mechanical effects of injections. Bath application of DHβE (0.1–0.5 μM) greatly reduced the amplitude and duration of the tonic/seizure-like activity induced by microinjection of nicotine into the ipsilateral XII nucleus to 2.9 ± 2.3 μV ($p = 0.028$, paired t test, $n = 7$) and 6.8 ±

4.7 s ($p = 0.002$), respectively (Fig. 6C2,C3). In the presence of DHβE, nicotine injection into the ipsilateral XII nucleus has no effect on frequency (7.6 ± 2.2/min in prenicotine conditions vs 7.3 ± 1.8/min after nicotine injection, $p = 0.89$, $n = 7$) or on amplitude (11.9 ± 6.4 μV vs 11.8 ± 6.1 μV, $p = 0.97$) of the integrated XIIn rhythmic activity (Fig. 6C1).

These results suggest that functional α4* nAChRs are present both in the pre-BötC and the XII nucleus. However, the effects of activating these receptors differ: α4* nAChRs in the preBötC mediate ACh/nicotinic modulation of respiratory frequency, and α4* nAChRs in the XII nucleus mediate ACh/nicotine induced tonic/seizure-like activity in XIIn.

Discussion

This study demonstrates several points related to nicotinic receptor composition and its function in the neural control of respiration. (1) The concentration–response relationship of respiratory rhythm in L9′A mice was greatly shifted to lower nicotine concentrations compared with that in wild-type mice *in vitro*. Respiratory frequency in predrug control conditions in L9′A mice was higher than that of wild-type mice, suggesting that the respiratory rhythm of L9′A mice is hypersensitive to nicotine and endogenous ACh. (2) Responses induced by 5 nM nicotine in pre-BötC inspiratory neurons and respiratory-related XIIn rhythmic activity in L9′A mice resembled 1 μM nicotine-induced responses in wild-type mice. These responses included (i) depolarization of current-clamped inspiratory neurons; (ii) a tonic inward current in voltage-clamped inspiratory neurons associated with an increase in membrane noise; (iii) a decrease in phasic inspiratory drive current; (iv) an increase in frequency and amplitude of sEPSCs; and (v) an increase in respiratory

frequency and tonic/seizure-like activity in XIIn rhythmic motor output. These data suggest that a substantial fraction of the nAChRs mediating the nicotinic effects on inspiratory neurons in the preBötC rhythmogenic network contain α4 subunits. Nicotine, via activation of α4* nAChRs, facilitates glutamatergic excitatory input to preBötC inspiratory neurons and depolarizes these neurons, resulting in increased respiratory frequency. (3) Microinjection of nicotine at low nanomolar concentrations into the preBötC in L9′A slices increased respiratory frequency, and injection into the ipsilateral XII nucleus induced tonic/seizure-like activity. These results suggest that functional α4* nAChRs are present in the preBötC and XII nucleus. Because nicotine at these low concentrations does not activate non-α4* nAChRs, we conclude that activation of α4* nAChRs in the preBötC is sufficient for nicotine-induced increase in respiratory rhythm and also that activation of α4* receptors in XII nucleus is sufficient for the nicotine-induced increase in tonic motor activity in XIIn. (4) The

α4*-selective nAChR antagonist DHβE blocked the effects of nicotine, suggesting that α4* nAChRs mediate the nicotine effect. Furthermore, in L9′A mice, DHβE alone induced effects opposite to those of nicotine on preBötC inspiratory neurons and respiratory-related XIIn rhythmic activity. DHβE induced (i) an outward current associated with a decrease in membrane noise; (ii) a decrease in sEPSC frequency and amplitude; and (iii) a decrease in respiratory frequency. These effects of DHβE suggest that the hypersensitive receptors are continually activated by endogenous ACh (Shao and Feldman, 2007b). In summary, the results of this study suggest that α4* nAChRs in the preBötC play key functional roles in mediating cholinergic/nicotinic modulation of the excitability of inspiratory neurons and modulation of respiratory rhythm. α4* nAChRs in the XII nucleus play key roles in mediating cholinergic/nicotinic modulation of tonic activity in XIIn. These results are consistent with our previous pharmacological study (Shao and Feldman, 2002) and provide further evidence for the molecular composition of the nAChRs mediating the cholinergic/nicotinic modulation of respiratory pattern. We do not exclude the possibility that other subtypes of nAChRs also exist in the preBötC and XII nucleus and play a role in cholinergic modulation of the respiratory pattern.

We comment on the subunit composition of the α4* receptors studied here. Our oocyte expression methods were optimized for expression of α4L9′A receptors with $(\alpha 4)_2(\beta 2)_3$ stoichiometry (X. Xiu, N. Puskar, D. Dougherty, and H. A. Lester, unpublished results). Wild-type receptors and α4-M2 mutant receptors exist in both $(\alpha 4)_2(\beta 2)_3$ and $(\alpha 4)_3(\beta 2)_2$ forms, in mice as well as in heterologous expression systems. These two forms of α4β2 receptors have distinct sensitivities to both agonists and antagonists. The $(\alpha 4)_2(\beta 2)_3$ stoichiometry is thought to display the higher sensitivity to ACh, nicotine, and DHβE (Moroni et al., 2006). The substantial effects of presumably modest extracellular ACh levels, and the nearly complete blockade by 0.2 μM DHβE, suggest that the nAChRs underlying the nicotinic modulation of respiratory pattern, detected in our experiments, are the high-sensitivity $(\alpha 4)_2(\beta 2)_3$ type. However, because other subunits may also be present in the preBötC or XII nucleus, it is premature to make definite conclusions about the precise stoichiometry. For example, α4β4* receptors are also very sensitive to blockade by DHβE. However, β4 subunit expression has not been seen in these regions in neonatal and adult rats (Dineley-Miller and Patrick, 1992; Zoli et al., 1995; Winzer-Serhan and Leslie, 1997).

Nicotine alters the excitability of preBötC inspiratory neurons via α4* nAChRs

Taking advantage of the genetically engineered L9′A mouse strain, we were able to activate specifically the α4* nAChRs with low nanomolar concentrations of nicotine (Tapper et al., 2004; Fonck et al., 2005). Because the sEPSCs and the phasic inspiratory drive current are not blocked by DHβE or other AChR antagonists [such as nicotinic antagonists mecamylamine, methyllycaconitine, and muscarinic antagonist atropine (Shao and Feldman, 2000, 2001, 2002)] but can be completely blocked by 6-cyano-7-nitroquinoxaline-2,3-dione, they are glutamatergic EPSCs from excitatory synapses on the preBötC inspiratory neurons (Shao and Feldman, 2001). The results in this study that nicotine at low nanomolar concentrations increased the frequency and amplitude of sEPSCs, whereas DHβE decreased them in L9′A mice, suggest that nicotine or ambient levels of ACh [volume transmission (Zoli et al., 1999; Dani and Bertrand, 2007)] facilitate glutamatergic transmission by activation of α4*

nAChRs on presynaptic sites and/or upstream to the synaptic boutons [including preterminal nAChRs (Lena et al., 1993)] of neurons that send excitatory input to preBötC inspiratory neurons. The results that nicotine induced a tonic inward current associated with an increase in membrane noise in inspiratory neurons could arise from activation of postsynaptic and/or extrasynaptic nAChRs in addition to facilitation of glutamatergic transmission. Our results in current study do not exclude the possibility that activation of postsynaptic and/or extrasynaptic α4* nAChRs by nicotine or by ambient levels of ACh may also contribute to modulation of the excitability of the postsynaptic neurons. Increase in excitability and depolarization of preBötC inspiratory neurons results in an increase in respiratory frequency.

Nicotine sensitivity of wild-type rodents and L9′ mutant mice

Our data indicate that nicotine is less potent in modulating respiratory rhythm in neonatal C57BL/6 mice (wild-type) than Sprague Dawley rats of similar ages. In Sprague Dawley neonatal rats, respiratory frequency in slices increases by 188 ± 28% with 0.2 μM nicotine and by 280 ± 61% with 0.5 μM nicotine (Shao and Feldman, 2001). In wild-type C57BL/6 neonatal mice in this study, respiratory frequency increased by 119.1 ± 15.9% with 0.5 μM and by 147.7 ± 19.8% with 1 μM nicotine (Fig. 1C). There are clearly species differences in cholinergic/nicotinic modulation of respiratory rhythm.

Although nicotine is less potent in wild-type mice, the L9′A mutation on the α4* nAChRs renders nicotine ~100-fold more potent to induce cellular and systemic respiratory responses. This increase in sensitivity agrees well with similar increases measured for L9′A receptors expressed in oocytes (Fonck et al., 2005), for nicotine-induced Ca^{2+} increases in neurons from L9′A mice (Tapper et al., 2004; Fonck et al., 2005), and for nicotine-induced hypothermia in L9′A mice (Tapper et al., 2004, 2007). In neonatal wild-type rats, application of DHβE alone does not affect preBötC neurons and the respiratory rhythm, probably because of low concentrations of background ACh release under *in vitro* conditions (Shao and Feldman, 2005). However, in L9′A mice, DHβE induced effects opposite to nicotine application, suggesting that the L9′A nAChRs are sensitive to the endogenous ambient levels of ACh (Shao and Feldman, 2007b) and that these α4* nAChRs are not completely desensitized by the endogenous ligands, consistent with the finding that the hypersensitive receptors have a "window" of activation in the sustained presence of agonist (Fonck et al., 2005). Therefore, blockade of these L9′A receptors antagonizes the endogenous ACh actions on preBötC inspiratory neurons and the respiratory rhythm, resulting in opposite effects. This rather subtle effect of DHβE is the first report that endogenous ACh alone has a detectable effect in L9′A mice at the cellular level. However, L9′A mice do have a sleep disorder that could arise from endogenous ACh (Fonck et al., 2005). An even more hypersensitive strain, L9′S, is so hypersensitive to endogenous agonists that their seizure threshold to anticholinesterase drugs is significantly lower than that of wild-type mice (Fonck et al., 2003).

nAChRs in XII nucleus

Hypoglossal motoneurons innervate the tongue and upper airway muscles (Aldes, 1995; Dobbins and Feldman, 1995) and play an important role in regulating upper airway resistance and patency (Fuller et al., 1999). Immunoreactivity for α4 and α7 nAChR subunits is present in the XII nucleus (Dominguez del Toro et al., 1994; Dehkordi et al., 2005). β2 subunit mRNA is also

detectable (Wada et al., 1989). Activation of nAChRs excites hypoglossal motoneurons (Zaninetti et al., 1999; Chamberlin et al., 2002; Robinson et al., 2002; Quitadamo et al., 2005). In this study, we illustrated that functional α4* nAChRs were expressed in the XII nucleus and that selective activation of these receptors enhanced tonic activity without affecting the amplitude and duration of inspiratory bursts of XIIn motor output. Activation of α4* nAChRs likely depolarizes hypoglossal motoneurons (Zaninetti et al., 1999; Chamberlin et al., 2002), resulting in tonic spiking that underlies the tonic/seizure-like activity in XIIn. These results suggest that nAChRs in the XII nucleus play key functional roles in modulating the respiratory-related motor activity of XIIn, whereas α4* nAChRs primarily contribute to the mediation of the cholinergic regulation of upper airway tone. These results (Fig. 6) are consistent with those of Fonck et al. (2005) and suggest that cholinergic modulation of motoneuronal excitability via α4* nAChRs may, partially, underlie hypersensitivity of L9′A mice to nicotine-induced seizures.

References

Aldes LD (1995) Subcompartmental organization of the ventral (protrusor) compartment in the hypoglossal nucleus of the rat. J Comp Neurol 353:89–108.

Anderson ME, Johnson DC, Batal HA (2005) Sudden Infant Death Syndrome and prenatal maternal smoking: rising attributed risk in the Back to Sleep era. BMC Med 3:4.

Bellingham MC, Ireland MF (2002) Contribution of cholinergic systems to state-dependent modulation of respiratory control. Respir Physiol Neurobiol 131:135–144.

Chamberlin NL, Bocchiaro CM, Greene RW, Feldman JL (2002) Nicotinic excitation of rat hypoglossal motoneurons. Neuroscience 115:861–870.

Champtiaux N, Changeux JP (2004) Knockout and knockin mice to investigate the role of nicotinic receptors in the central nervous system. Prog Brain Res 145:235–251.

Clements JD, Bekkers JM (1997) Detection of spontaneous synaptic events with an optimally scaled template. Biophys J 73:220–229.

Dani JA, Bertrand D (2007) Nicotinic acetylcholine receptors and nicotinic cholinergic mechanisms of the central nervous system. Annu Rev Pharmacol Toxicol 47:699–729.

Dehkordi O, Haxhiu MA, Millis RM, Dennis GC, Kc P, Jafri A, Khajavi M, Trouth CO, Zaidi SI (2004) Expression of alpha-7 nAChRs on spinal cord-brainstem neurons controlling inspiratory drive to the diaphragm. Respir Physiol Neurobiol 141:21–34.

Dehkordi O, Millis RM, Dennis GC, Coleman BR, Johnson SM, Changizi L, Ovid Trouth C (2005) Alpha-7 and alpha-4 nicotinic receptor subunit immunoreactivity in genioglossus muscle motoneurons. Respir Physiol Neurobiol 145:153–161.

Dineley-Miller K, Patrick J (1992) Gene transcripts for the nicotinic acetylcholine receptor subunit, beta4, are distributed in multiple areas of the rat central nervous system. Brain Res Mol Brain Res 16:339–344.

Dobbins EG, Feldman JL (1995) Differential innervation of protruder and retractor muscles of the tongue in rat. J Comp Neurol 357:376–394.

Dominguez del Toro E, Juiz JM, Peng X, Lindstrom J, Criado M (1994) Immunocytochemical localization of the α7 subunit of the nicotinic acetylcholine receptor in the rat central nervous system. J Comp Neurol 349:325–342.

Feldman JL, Mitchell GS, Nattie EE (2003) Breathing: rhythmicity, plasticity, chemosensitivity. Annu Rev Neurosci 26:239–266.

Fonck C, Nashmi R, Deshpande P, Damaj MI, Marks MJ, Riedel A, Schwarz J, Collins AC, Labarca C, Lester HA (2003) Increased sensitivity to agonist-induced seizures, Straub tail, and hippocampal theta rhythm in knock-in mice carrying hypersensitive α4 nicotinic receptors. J Neurosci 23:2582–2590.

Fonck C, Cohen BN, Nashmi R, Whiteaker P, Wagenaar DA, Rodrigues-Pinguet N, Deshpande P, McKinney S, Kwoh S, Munoz J, Labarca C, Collins AC, Marks MJ, Lester HA (2005) Novel seizure phenotype and sleep disruptions in knock-in mice with hypersensitive α4* nicotinic receptors. J Neurosci 25:11396–11411.

Fuller DD, Williams JS, Janssen PL, Fregosi RF (1999) Effect of co-

activation of tongue protrudor and retractor muscles on tongue movements and pharyngeal airflow mechanics in the rat. J Physiol (Lond) 519:601–613.

Gotti C, Riganti L, Vailati S, Clementi F (2006) Brain neuronal nicotinic receptors as new targets for drug discovery. Curr Pharm Des 12:407–428.

Gray PA, Rekling JC, Bocchiaro CM, Feldman JL (1999) Modulation of respiratory frequency by peptidergic input to rhythmogenic neurons in the preBötzinger complex. Science 286:1566–1568.

Harvey SC, Luetje CW (1996) Determinants of competitive antagonist sensitivity on neuronal nicotinic receptor β subunits. J Neurosci 16:3798–3806.

Harvey SC, Maddox FN, Luetje CW (1996) Multiple determinants of dihydro-β-erythroidine sensitivity on rat neuronal nicotinic receptor α subunits. J Neurochem 67:1953–1959.

Kinney HC, Filliano JJ, Sleeper LA, Mandell F, Valdes-Dapena M, White WF (1995) Decreased muscarinic receptor binding in the arcuate nucleus in sudden infant death syndrome. Science 269:1446–1450.

Labarca C, Schwarz J, Deshpande P, Schwarz S, Nowak MW, Fonck C, Nashmi R, Kofuji P, Dang H, Shi W, Fidan M, Khakh BS, Chen Z, Bowers BJ, Boulter J, Wehner JM, Lester HA (2001) Point mutant mice with hypersensitive α4 nicotinic receptors show dopaminergic deficits and increased anxiety. Proc Natl Acad Sci USA 98:2786–2791.

Lena C, Changeux JP, Mulle C (1993) Evidence for "preterminal" nicotinic receptors on GABAergic axons in the rat interpeduncular nucleus. J Neurosci 13:2680–2688.

Liu G, Feldman JL, Smith JC (1990) Excitatory amino acid-mediated transmission of inspiratory drive to phrenic motoneurons. J Neurophysiol 64:423–436.

Mitchell EA, Milerad J (2006) Smoking and the sudden infant death syndrome. Rev Environ Health 21:81–103.

Moroni M, Zwart R, Sher E, Cassels BK, Bermudez I (2006) α4β2 nicotinic receptors with high and low acetylcholine sensitivity: pharmacology, stoichiometry, and sensitivity to long-term exposure to nicotine. Mol Pharmacol 70:755–768.

Nicholson C (1985) Diffusion from an injected volume of a substance in brain tissue with arbitrary volume fraction and tortuosity. Brain Res 333:325–329.

Picciotto MR, Caldarone BJ, Brunzell DH, Zachariou V, Stevens TR, King SL (2001) Neuronal nicotinic acetylcholine receptor subunit knockout mice: physiological and behavioral phenotypes and possible clinical implications. Pharmacol Ther 92:89–108.

Quitadamo C, Fabbretti E, Lamanauskas N, Nistri A (2005) Activation and desensitization of neuronal nicotinic receptors modulate glutamatergic transmission on neonatal rat hypoglossal motoneurons. Eur J Neurosci 22:2723–2734.

Robinson DM, Peebles KC, Kwok H, Adams BM, Clarke LL, Woollard GA, Funk GD (2002) Prenatal nicotine exposure increases apnoea and reduces nicotinic potentiation of hypoglossal inspiratory output in mice. J Physiol (Lond) 538:957–973.

Shao XM, Feldman JL (2000) Acetylcholine modulates respiratory pattern: effects mediated by M3-like receptors in preBötzinger complex inspiratory neurons. J Neurophysiol 83:1243–1252.

Shao XM, Feldman JL (2001) Mechanisms underlying regulation of respiratory pattern by nicotine in preBötzinger Complex. J Neurophysiol 85:2461–2467.

Shao XM, Feldman JL (2002) Pharmacology of nicotinic receptors in pre-Bötzinger Complex that mediate modulation of respiratory pattern. J Neurophysiol 88:1851–1858.

Shao XM, Feldman JL (2005) Cholinergic neurotransmission in the pre-Bötzinger Complex modulates excitability of inspiratory neurons and regulates respiratory rhythm. Neuroscience 130:1069–1081.

Shao XM, Feldman JL (2007a) Micro-agar salt bridge in patch-clamp electrode holder stabilizes electrode potentials. J Neurosci Methods 159:108–115.

Shao XM, Feldman JL (2007b) Efficient measurement of endogenous neurotransmitters in small localized regions of central nervous systems in vitro with HPLC. J Neurosci Methods 160:256–263.

Smith JC, Ellenberger HH, Ballanyi K, Richter DW, Feldman JL (1991) Pre-Bötzinger complex: a brainstem region that may generate respiratory rhythm in mammals. Science 254:726–729.

Tapper AR, McKinney SL, Nashmi R, Schwarz J, Deshpande P, Labarca C,

Whiteaker P, Marks MJ, Collins AC, Lester HA (2004) Nicotine activation of α4* receptors: sufficient for reward, tolerance, and sensitization. Science 306:1029 –1032.

Tapper AR, McKinney SL, Marks MJ, Lester HA (2007) Nicotine responses in hypersensitive and knockout α4 mice account for tolerance to both hypothermia and locomotor suppression in wild-type mice. Physiol Genomics 31:422– 428.

Wada E, Wada K, Boulter J, Deneris E, Heinemann S, Patrick J, Swanson LW (1989) Distribution of alpha 2, alpha 3, alpha 4, and beta 2 neuronal nicotinic receptor subunit mRNAs in the central nervous system: a hybridization histochemical study in the rat. J Comp Neurol 284:314 –335.

Whiteaker P, Cooper JF, Salminen O, Marks MJ, McClure-Begley TD, Brown RW, Collins AC, Lindstrom JM (2006) Immunolabeling demonstrates the interdependence of mouse brain α4 and β2 nicotinic acetylcholine receptor subunit expression. J Comp Neurol 499:1016 –1038.

Winzer-Serhan UH, Leslie FM (1997) Codistribution of nicotinic acetylcholine receptor subunit α3 and β4 mRNAs during rat brain development. J Comp Neurol 386:540 –554.

Zaninetti M, Tribollet E, Bertrand D, Raggenbass M (1999) Presence of functional neuronal nicotinic acetylcholine receptors in brainstem motoneurons of the rat. Eur J Neurosci 11:2737 –2748.

Zoli M, Le Novere N, Hill Jr JA, Changeux JP (1995) Developmental regulation of nicotinic ACh receptor subunit mRNAs in the rat central and peripheral nervous systems. J Neurosci 15:1912 –1939.

Zoli M, Jansson A, Sykova E, Agnati LF, Fuxe K (1999) Volume transmission in the CNS and its relevance for neuropsychopharmacology. Trends Pharmacol Sci 20:142 –150.